AJNR

Tractography for Arteriovenous Malformations Near the Sensorimotor Cortices

Kei Yamada, Osamu Kizu, Hirotoshi Ito, Takao Kubota, Wataru Akada, Mariko Goto, Akihiro Takada, Jyunya Konishi, Hiroyasu Sasajima, Katsuyoshi Mineura, Susumu Mori and Tsunehiko Nishimura

Technical Note ——————————————————————

Tractography for Arteriovenous Malformations Near the Sensorimotor Cortices

Kei Yamada, Osamu Kizu, Hirotoshi Ito, Takao Kubota, Wataru Akada, Mariko Goto, Akihiro Takada, Jyunya Konishi, Hiroyasu Sasajima, Katsuyoshi Mineura, Susumu Mori, and Tsunehiko Nishimura

Summary: We sought to use diffusion-tensor imaging–based tractography to assess the relationship between the arteriovenous malformations (AVM) and the sensorimotor cortices/tracts. Three patients who had an AVM closely situated to the sensorimotor tracts were studied. The relationship between the sensorimotor tracts and the AVM was well demonstrated in all patients. Tractography was also helpful in identifying the location of the motor cortex in some of the cases.

Surgical management of arteriovenous malformation (AVM) has a high risk when eloquent areas of the brain are involved (1). Therefore, knowing the precise location of these areas and their axonal pathways would enable safer surgery. Fiber-tracking method is a relatively new neuroimaging technique that visualizes 3D macroscopic fiber orientation in the brain (2–4). We applied this technique to patients with nonhemorrhagic AVMs that were in close proximity to the sensorimotor cortices to examine its clinical impact.

Materials and Methods

Patient Population

This study was approved by an institutional review board, and written informed consent was obtained from each patient. We performed MR imaging on 18 consecutive patients who presented to our institute with nonhemorrhagic intracranial AVM, during the study period between August 2001 and December 2002. Among these 18 consecutive patients, three patients had lesions closely situated to the sensorimotor cortices. All three patients had been conservatively followed because of their high scores on the Spetzler-Martin grading system (1). The demographic data of the patients are summarized in Table 1.

Imaging Methods

Thin-section diffusion-tensor imaging was performed at the end of our routine brain protocol. The diffusion-tensor image acquisition time was 4 minutes and 24 seconds. Images were obtained by using a 1.5-T whole-body scanner (Gyroscan Intera, Philips Medical Systems, Best, the Netherlands). A single-shot echo-planar imaging (EPI) technique was used for the diffusion-tensor image (repetition time/*echo* time = 6000/88 ms) with a motion-probing gradient in six orientations, a b value of 800 s/mm^2, and image averaging of six times. The recorded data points were 128×53 by using the parallel imaging technique. The parallel imaging technique allows for image reconstruction by using half the encoding steps, the advantage of which lies in its reduction of the geometric image distortion that is unique to EPI. The true resolution of the acquired images was equivalent to 128×106. The data were zero filled to generate images with 128×128 resolution. A total of 36 sections were obtained with a thickness of 3 mm without interslice gaps.

Data Processing

We transferred the diffusion-tensor imaging data to an off-line workstation for analysis. Data were analyzed with a PRIDE (Philips Research Integrated Development Environment) software written in Interactive Data Language (RSI, Inc, Boulder, CO). Diffusion tensor elements, including vectors and anisotropy at each voxel were calculated by using method described elsewhere (5–7). The primary direction of the principal eigenvector of the diffusion tensor at each location tends to be along the direction of the fiber passing through that location. This is because water diffuses preferentially along the axis of these principal eigenvectors, thus generating trajectories of fiber bundles. Starting from a particular region of interest, one can follow the direction of the principal eigenvector, thus following the corresponding fiber. Translation of eigenvectors into neuronal trajectories was achieved by a technique known as the fiber assignment by continuous tracking (FACT) method, which was initially described by Mori et al (2).

The procedure for mapping neural connections is started by designating two arbitrary regions of interest in the 3D space on PRIDE software. The region of interest placement typically starts at the brain stem (Fig 1). If this process depicts fiber tracts that terminate at the sensorimotor cortices, the process stops here. If there were too many fiber tracts that reached areas other than the target cortices, we added another region of interest at the sensorimotor cortices to be more specific. These additional regions of interest were, however, placed only when the sensorimotor cortices were reliably identified based on the sulcal pattern on transaxial images at the vertex. In this study, regions of interest at the sensorimotor cortices were not used for cases 1 and 2 because the nidi of the AVMs were situated close to the sensorimotor cortices, causing distortion of the brain architecture.

Tracking was terminated when it reached a pixel with low fractional anisotropy (FA < 0.3) or a predetermined trajectory curvature between two contiguous vectors (inner product < 0.85). Fiber tracts that passed through both regions of interest

Demographic data of the patients

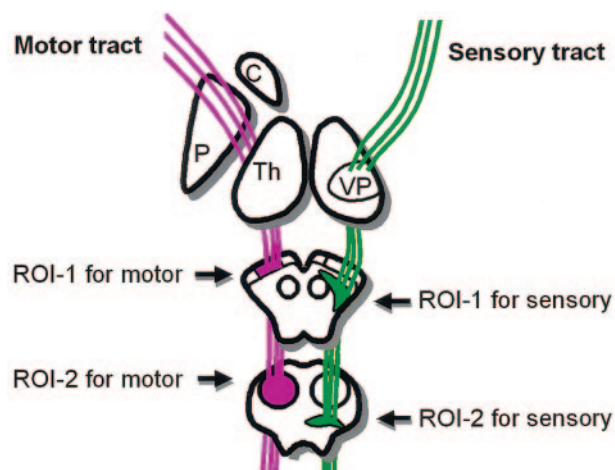| Patient	Age	Sex	Side	Symptom	Eloquence	Size (mm)	Deep veins	Spetzler-Martin grading
1	53	M	right	none	sensorimotor	52 × 43 × 60	yes	IV
2	28	F	left	extremity seizure	sensorimotor	38 × 42 × 45	yes	IV
3	59	M	both	none	sensorimotor	35 × 37 × 45	yes	IV

FIG 1. Schematic drawing of a typical region of interest setting for sensory and motor tractography.

were designated to be the final tract of interest. The traced fiber tracts in this study included the motor and sensory pathways. A typical tract reconstruction by using a two–region of interest method required approximately 1 minute by using a 2.66-GHz Pentium IV workstation (Dell, Austin, TX). The entire data postprocessing time for sensorimotor tracts on both hemispheres took approximately 10–15 minutes after completion of the examination, including the data transfer to the off-line workstation.

Results

Tractography was successfully obtained in all three patients. The relationship between sensorimotor tracts and the nidi were clearly depicted in all patients. In two of three patients, the location of the sensorimotor cortices was difficult to discern because of distorted brain architecture (Figs 2 and 3). In these two patients, tractography generated by placing seed points at the brain stem was able to locate the sensorimotor cortices. In
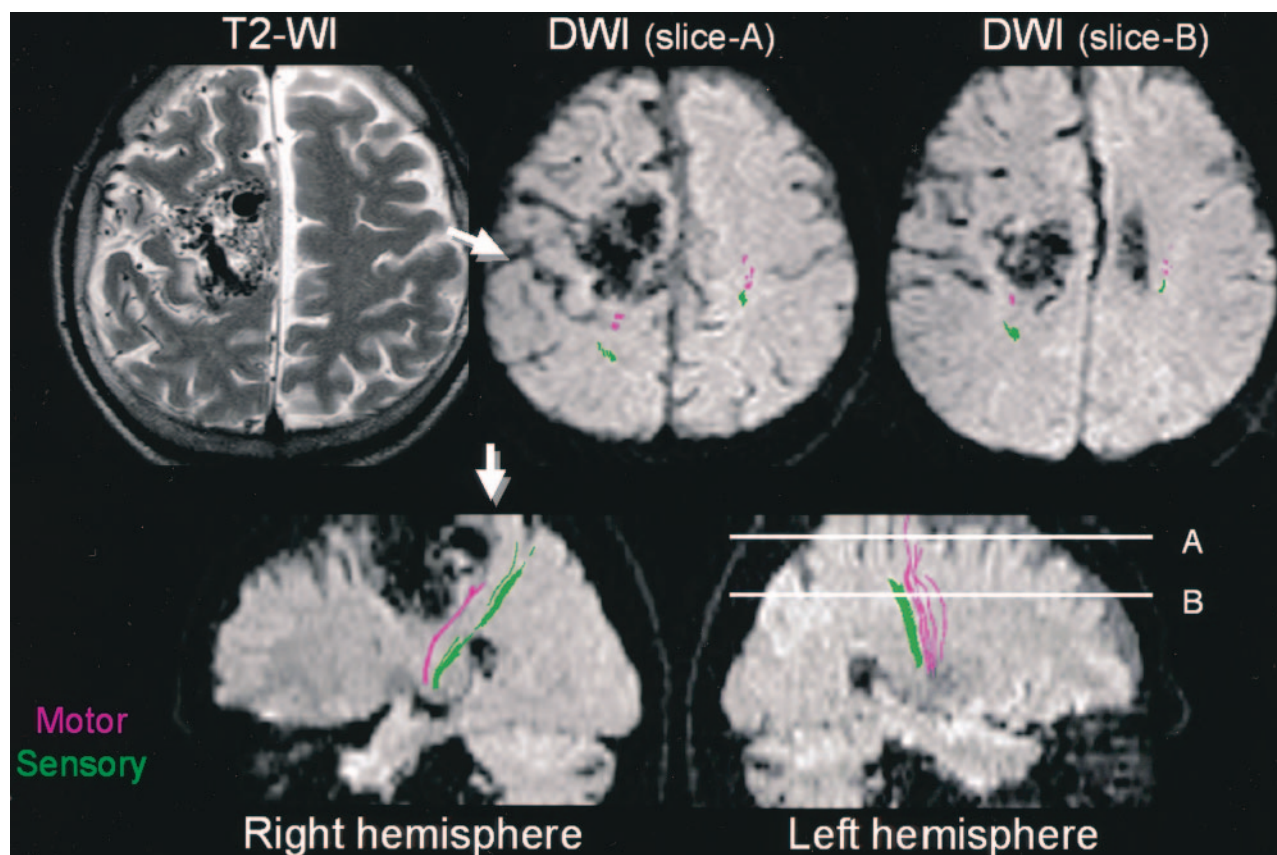

FIG 2. Patient 1, a 53-year-old patient without significant clinical symptoms. The patient has a large nidus of AVM involving the right frontoparietal region with obliteration of cortical sulci, which made it difficult to identify the motor cortex. Tractography clearly depicted the motor tract as being deviated posterior to the nidus. The location of the central sulcus could now be identified by using tractography as a landmark (*arrows*).
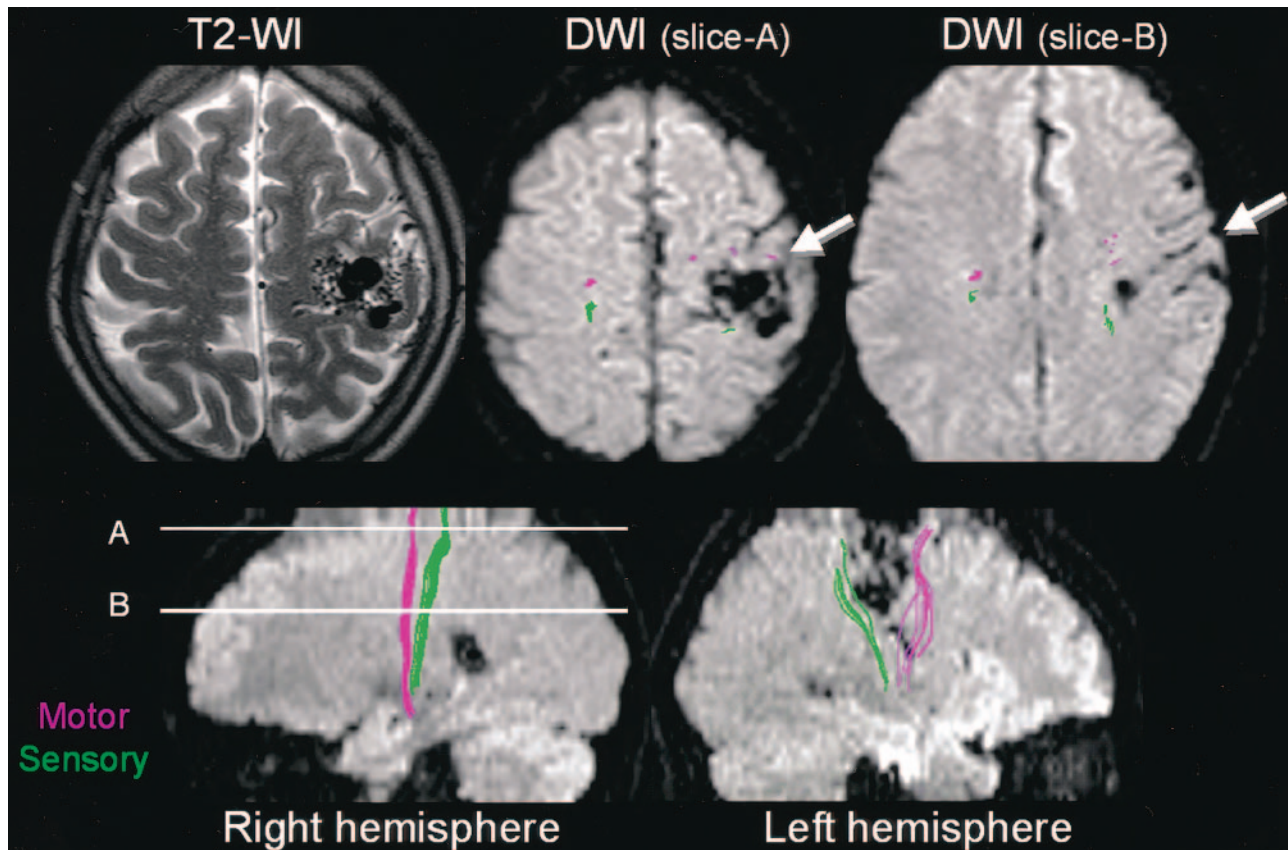
FIG 3.   Patient 2, a 28-year-old patient with a right extremity seizure. An AVM is noted to be closely situated to the area of sensorimotor cortices. Tractography showed the motor tract to be located anterior to the nidus and the sensory tract to be located posterior to the nidus. The deep draining vein at section *B* is in close proximity to both the motor and the sensory tracts. The motor tract is noted anterior to this vessel.

both patients the sensorimotor cortices were significantly deviated from their normal location.

Tractography was able to depict not only the locations of the eloquent cortices, but also that of the eloquent "tracts." The correlation between these tracts and the nidi or its draining vessels could be assessed in 3D space, as shown in Figs 2–4. Multiple draining vessels were noted in patient 3 (Fig 4); one of these, the right deep draining vein, traveled along the lateral wall of the right lateral ventricle and was shown to be in close proximity to the motor tract, whereas the left deep draining vein was shown to cross dorsal to the sensory tract (Fig 4B).

Discussion

In this study, we have shown that tractography is a clinically feasible technique that enables the *in vivo* evaluation of eloquent fiber tracts and cortices. All three patients presented in this report had AVMs that were situated close to the sensorimotor pathways, and all of these were clearly depicted by using tractography. This technique provided information that was thought to be clinically important and that is virtually impossible to obtain through conventional anatomical MR imaging studies, such as T1- and T2-weighted images.

This method uses information obtained from diffusion anisotropy that can be recorded by the diffusion-tensor imaging technique. The acquired data can be postprocessed to reflect the propensity of water molecule diffusion within a pixel, as the diffusion perpendicular to the nerve axis will be limited by the cell membrane and the myelin sheaths, whereas diffusion along the nerve axis is less limited. This imaging technique has become progressively common in the past few years, and it can now be performed with most of the recent commercially available MR scanners (8).

Depending on the clinical needs, tractography can be used to assess AVMs in two different ways. First, it can be used to locate the eloquent cortices, which would be especially helpful when there is significant distortion in normal brain architecture, making it difficult to discern the sulci of the frontoparietal areas. This task can be accomplished by placing the seed regions of interest in areas located away from the target cortex of interest (Fig 1). Such patients, in whom the regions of interest for identifying the sensorimotor cortices were placed at the midbrain and pons, are depicted in Figures 2 and 3.

The second way that this technique can be used is to delineate the relationship between the white matter pathways and the nidi or their deep draining vessels. Depicting the sensorimotor pathways at the
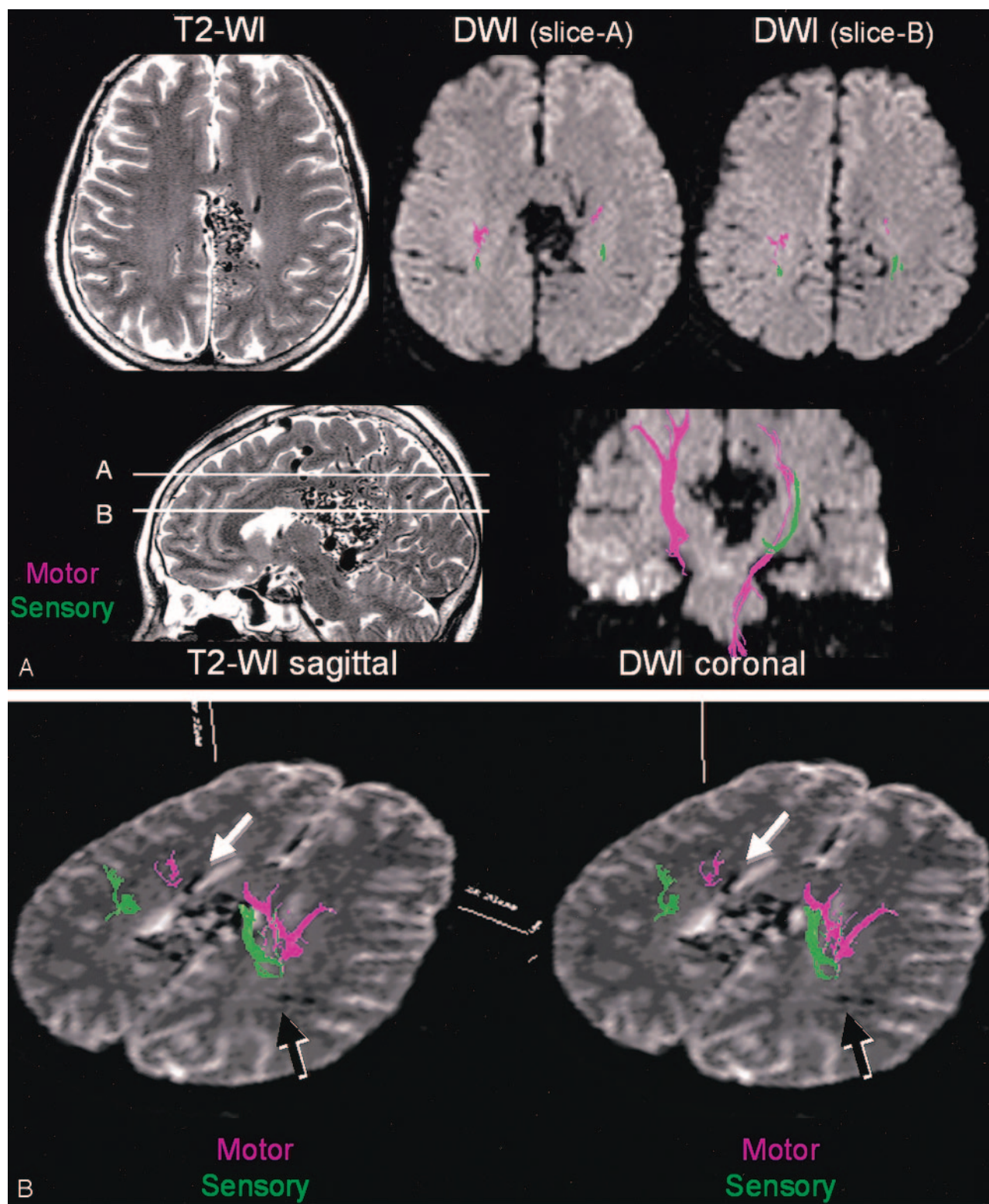
FIG 4. Patient 3, a 59-year-old without significant clinical symptoms. A large AVM is noted around the splenium of the corpus callosum. The main body of the nidus is in close proximity to the sensorimotor tracts, especially at the medial aspect of the left hemisphere. B, Stereo view from above shows multiple draining veins around the lesion, some of which are situated close to the sensorimotor tracts. For instance, the left deep draining vein along the lateral ventricle is shown to be in close proximity to the motor tract (*white arrow*). The right deep draining vein is shown to cross dorsal to the sensory tract (*black arrow*).

centrum semiovale can be especially important when there are deep draining and feeding vessels that are closely situated to these eloquent tracts. The centrum

semiovale, however, has few surgical landmarks that enable the identification of these sensorimotor tracts, and assessment has relied mainly on intraoperative

electrophysiologic tests. It would be of great benefit to know a priori the course of these eloquent tracts, because this would help in choosing the direction of the surgical approach, as well as in guiding the surgeon to the areas where the most meticulous maneuvering may be necessary.

Because all the lesions examined in this study were not only located at the eloquent areas but also had a large size and deep draining veins, they were determined to have a high surgical risk (Spetzler-Martin grade IV). Therefore, none of these patients had undergone surgical lesion removal. Consequently, the direct surgical impact of the technique described in this article that can depict sensorimotor tracts remains to be proved in future studies. The utilization of this technique in patients with lesions amenable to surgical intervention (Spetzler-Martin grades I–III) will be the next step of our research.

A few technical issues deserve comment. A previous tractography study has shown that vasogenic edema surrounding brain tumors hampers the depiction of eloquent tracts by using this technique (8). This failure occurs because the diffusion anisotropy decreases within the areas where there is vasogenic edema. This is not typically seen in cases with a nonhemorrhagic AVM, however, because they tend to have much less significant vasogenic edema around the lesion, as compared with patients with brain tumors. Thus, we believe that this method is feasible for most patients with nonhemorrhagic cerebral AVMs. In patients with an acute hemorrhage, technical difficulty may occur when performing fiber tracking, not only because of the edema surrounding the lesion, but also possibly because of susceptibility artifact from the hematoma, which may cause signal intensity drop off around the nidus on the source diffusion-tensor image.

There are a few other technical limitations that are known to occur with this fiber-tracking technique. First, image acquisition by using single-shot EPI techniques results in an inherently limited spatial resolution and also subjects the images to distortion and susceptibility effects. Using multishot EPI or the propeller technique (9, 10) can resolve these problems, but at the expense of much longer imaging time. Second, tractography is only capable of depicting part of the tract. This is due in part to the above-mentioned limited spatial resolution and to a phenomenon known as the "crossing-fiber problem" that also limits this technique. A detailed description of this issue is beyond the scope of the article and can be found elsewhere (11, 12). It is, however, expected to be solved by means of more sophisticated imaging techniques (11, 12).

Despite the above-mentioned technical limitation, the image quality of our current tractography is thought to be satisfactory, and the diffusion-tensor imaging time is short enough, making it a readily applicable technique for routine clinical imaging. Furthermore, the postprocessing time required to obtain preliminary tractography is also short enough; it can be accomplished in approximately 10–15 minutes after completion of the examination. These times for data acquisition and postprocessing are considered to be acceptable for routine clinical use, even in the emergency setting.

Conclusion

Diffusion-tensor imaging–based MR tractography in patients with an AVM can not only identify the location of the eloquent cortex, but also depict the relationship between the tract, the nidus, and the deep veins. The information provided by this technique appears to have clinical applications. The next investigative step is to correlate the results of this technique with those of intraoperative electrophysiologic studies.

Acknowledgments

References

1. Spetzler RF, Martin NA. **A proposed grading system for arteriovenous malformations.** *J Neurosurg* 1986;65:476–483
2. Mori S, Crain BJ, Chacko VP, van Zijl PC. **Three-dimensional tracking of axonal projections in the brain by magnetic resonance imaging.** *Ann Neurol* 1999;45:265–269
3. Poupon C, Clark CA, Frouin V, et al. **Regularization of diffusion-based direction maps for the tracking of brain white matter fascicles.** *Neuroimage* 2000;12:184–195
4. Conturo TE, Lori NF, Cull TS, et al. **Tracking neuronal fiber pathways in the living human brain.** *Proc Natl Acad Sci U S A* 1999;96:10422–10427
5. Basser PJ, Mattiello J, LeBihan D. **Estimation of the effective self-diffusion tensor from the NMR spin echo.** *J Magn Reson B [B]* 1994;103:247–254
6. Pierpaoli C, Basser PJ. **Toward a quantitative assessment of diffusion anisotropy.** *Magn Reson Med* 1996;36:893–906
7. Makris N, Worth AJ, Sorensen AG, et al. **Morphometry of in vivo human white matter association pathways with diffusion-weighted magnetic resonance imaging.** *Ann Neurol* 1997;42:951–962
8. Yamada K, Kizu O, Mori S, et al. **Clinically feasible diffusion-tensor imaging for fiber tracking.** *Radiology* 2003;226:295–301
9. Brockstedt S, Moore JR, Thomsen C, et al. **High-resolution diffusion imaging using phase-corrected segmented echo-planar imaging.** *Magn Reson Imaging* 2000;18:649–657
10. Forbes KP, Pipe JG, Karis JP, Heiserman JE. **Improved image quality and detection of acute cerebral infarction with PROPELLER diffusion-weighted MR imaging.** *Radiology* 2002;225:551–555
11. Tuch DS, Reese TG, Wiegell MR, et al. **High angular resolution diffusion imaging reveals intravoxel white matter fiber heterogeneity.** *Magn Reson Med* 2002;48:577–582
12. Frank LR. **Anisotropy in high angular resolution diffusion-weighted MRI.** *Magn Reson Med* 2001;45:935–959.